Dissipative and dispersive behaviors of lattice-based models for hydrodynamics

Yue-Hong Qian[1,*] and Shi-Yi Chen[2]
[1]*Department of Applied Physics and Applied Mathematics, Columbia University, New York, New York 10027*
[2]*Center for Nonlinear Studies, Los Alamos National Laboratory, Los Alamos, New Mexico 87545*
(Received 22 January 1999)

Both dissipation and dispersion are present in many complex systems; their interactions through nonlinearity can lead to interesting features. We investigate in this paper the dissipation-dispersion interactions that exist in lattice-based kinetic models for hydrodynamics. The classical Chapman-Enskog expansion is used to derive the dispersion coefficients at third order of Knudsen number. Unlike the dissipation coefficient (viscosity) that is always *positive*, the dispersion coefficient can be either *positive* or *negative*. It would be interesting to know if there is any other physics in these models as compared with the traditional dispersionless Navier-Stokes dynamics. Traveling wave solutions in one dimension are studied and two different solutions have been found: (1) monotonic shock solutions and (2) oscillatory shock solutions, according to different conditions. In two- and three-dimensional systems, whether or not these oscillatory behaviors caused by the interactions between nonlinearity, dissipation, and dispersion have anything to do with vortex cascades (direct or inverse) would be an interesting question and we leave it for future studies.

PACS number(s): 47.11.+j, 51.10.+y

I. INTRODUCTION

For many complex systems we have to use computer simulations to understand some behaviors of the systems. Though computers become more and more powerful, lots of effort has been made to design simple and efficient numerical methods. A lattice-gas automata model introduced in 1986 is such a method to simulate hydrodynamics [1,2]. Lattice Bhatnagar-Gross-Krook models (lattice BGK) [3–5] was introduced to overcome some shortcomings of lattice-gas automata models while preserving strength. The advantages and disadvantages of the latter have been well studied [6,7].

It is generally believed that Boltzmann equation is more fundamental than hydrodynamic equations, and the classical kinetic theory provides a systematic derivation of the Euler, Navier-Stokes, Burnett, and super-Burnett equations as successive approximations of the Boltzmann equation in the order of Knudsen number ϵ [8]. The most difficult task in using the Burnett or super-Burnett equations is that additional boundary conditions are required to find the solutions, and there is no systematic way of imposing these additional conditions correctly [8].

In lattice-based models, it is also well established that the Navier-Stokes equation can be derived using the Chapman-Enskog expansion up to second order [2,3]. Many authors further asserted that the Burnett-like equation could be obtained by performing at higher order using the Chapman-Enskog expansion [2,7,9]. One motivation of this paper is to carry out these higher-order Chapman-Enskog expansions to investigate whether or not it is consistent to do so. Attention should be paid, however, when the classic Chapman-Enskog expansion is applied because of the noncommutative feature of cross derivatives of two time scales. The Burnett-like equations could be derived for lattice BGK models. The second motivation is to investigate the physical effects of these high-order terms since they exist in simulations. Since these high-order terms represent the dispersion, it is interesting to study the consequences of interactions between nonlinearity, dissipation, and dispersion, which are all present in many complex systems.

The paper is organized as follows. In Sec. II, we will derive the Burnett-like third-order equations, the corresponding equations for continuous time and space, but discrete velocity kinetic BGK models will be given in Sec. III; a linear dispersion relation and shock wave relations are presented in Sec. IV and Sec. V will offer a theoretical analysis of a traveling wave solution and its stability; numerical results will be shown in Sec. VI and the last section is for a discussion and concluding remarks.

II. CHAPMAN-ENSKOG EXPANSION: THIRD-ORDER HYDRODYNAMICS

The time evolution of lattice-based hydrodynamic models consists of two alternating substeps: neighbor-to-neighbor propagation of moving particles and collisional interaction of all particles at the same site. The starting equation is the following [4,10]

$$f_i(\vec{x}+\vec{c}_i,t+1)=f_i(\vec{x},t)+\omega[f_i^{\mathrm{eq}}(\vec{x},t)-f_i(\vec{x},t)], \qquad (1)$$

where f_i is the mean density of particles with discrete velocity $\vec{c}_i(i=0,1,2,\ldots,B)$, which belongs to a predetermined finite set and ω the relaxation parameter, which limits to $0 \leqslant \omega \leqslant 2$. The key point is how to choose the equilibrium density f_i^{eq} that depends only on the conserved and physically meaningful quantities. We use the same f_i^{eq} as that of Refs. [4], [10],

$$f_i^{\mathrm{eq}}=t_p\rho\left(1+\frac{c_{i\alpha}u_\alpha}{c_s}+\frac{(c_{i\alpha}c_{i\beta}-c_s^2\delta_{\alpha\beta})u_\alpha u_\beta}{2c_s^4}\right), \qquad (2)$$

*Present address: Exa Corporation, 450 Bedford Street, Lexington, MA 02420.

where c_s is a constant and t_p a weighting factor that are given in the following table for d-dimensional b velocity $DdQb$ models for the sake of self-containedness [3,4,10]:

Model	t_0	t_1	t_2	t_3	t_4	c_s^2
$D1Q3$	$\frac{2}{3}$	$\frac{1}{6}$	0	0	0	$\frac{1}{3}$
$D1Q5$	$\frac{1}{2}$	$\frac{1}{6}$	0	0	$\frac{1}{12}$	1
$D2Q7$	$\frac{1}{2}$	$\frac{1}{12}$	0	0	0	$\frac{1}{4}$
$D2Q9$	$\frac{4}{9}$	$\frac{1}{9}$	$\frac{1}{36}$	0	0	$\frac{1}{3}$
$D2Q13$	$\frac{2}{5}$	$\frac{8}{75}$	$\frac{1}{25}$	0	$\frac{1}{300}$	$\frac{2}{5}$
$D3Q15$	$\frac{2}{9}$	$\frac{1}{9}$	0	$\frac{1}{72}$	0	$\frac{1}{3}$
$D3Q19$	$\frac{1}{3}$	$\frac{1}{18}$	$\frac{1}{36}$	0	0	$\frac{1}{3}$
$D3Q33$	$\frac{43}{150}$	$\frac{4}{75}$	$\frac{2}{75}$	$\frac{1}{150}$	$\frac{1}{300}$	$\frac{2}{5}$
$D4Q25$	$\frac{1}{3}$	0	$\frac{1}{36}$	0	0	$\frac{1}{3}$

The hydrodynamic density ρ and velocity $\vec{u}$ are defined by

$$\sum_{i=0}^{B} f_i=\sum_{i=0}^{B} f_t^{\mathrm{eq}}=\rho, \quad \sum_{i=0}^{B} \vec{c}_i f_i=\sum_{i=0}^{B} \vec{c}_i f_i^{\mathrm{eq}}=\rho\vec{u}. \tag{3}$$

We assume a weak deviation from the local equilibrium $f_i^{\mathrm{eq}}(\vec{x},t)$,

$$f_i(\vec{x},t)=f_i^{\mathrm{eq}}(\vec{x},t)+\epsilon f_i^{(1)}(\vec{x},t)+\epsilon^2 f_i^{(2)}(\vec{x},t)+\cdots, \tag{4}$$

where ϵ is a small dimensionless number (Knudsen number). The space and time derivatives are expressed in terms of multiple-scale technique up to the third order in time,

$$\partial_\alpha=\epsilon\partial_\alpha, \tag{5}$$

$$\partial_t=\epsilon\partial_{t_1}+\epsilon^2\partial_{t_2}+\epsilon^3\partial_{t_3}. \tag{6}$$

In classical kinetic theory, Euler, Navier-Stokes, Burnett, and super-Burnett equations constitute the successive approximations of the Boltzmann equation in the order of Knudsen number ϵ. Like in classic kinetic theory, the lattice-based models for hydrodynamics use the Chapman-Enskog expansion in order to derive the large-scale dynamical equations. The basic ingredients of the derivation are the same as in Refs. [2, 3, 7, 11, 12]. The steps are as follows. (1) Use the double Taylor expansion in time and space of the evolution Eq. (1). (2) Replace the density f_i with the approximation (4). (3) Substitute the time and space derivatives with the multiple-scale technique (5) and (6). (4) Regroup terms in power orders of ϵ. (5) Sum over i and use the conservations (3). The conservation quantities lead to the constraints on high-order corrections $f_i^{(j)}$,

$$\sum_{i=0}^{B} f_i^{(j)}=0, \quad \sum_{i=0}^{B} \vec{c}_i f_i^{(j)}=0, \quad j>0. \tag{7}$$

The first-order ϵ equations are the inviscid Euler equations,

$$\partial_{t_1}\rho+\partial_\alpha(\rho u_\alpha)=0, \tag{8}$$

$$\partial_{t_1}(\rho u_\alpha)+\partial_\beta(\rho u_\alpha u_\beta)=-c_s^2\partial_\alpha\rho \tag{9}$$

and the second-order ϵ^2 yields the dissipative terms,

$$\partial_{t_2}\rho=0, \tag{10}$$

$$\partial_{t_2}(\rho u_\alpha)=\nu[\partial_{\beta\beta}(\rho u_\alpha)+\partial_{\alpha\beta}(\rho u_\beta)], \tag{11}$$

where ν is the shear viscosity $\{\nu=c^2/2[(2/\omega)-1]\}$.

At the third order ϵ^3, the Taylor expansion gives the following lengthy equation,

$$\begin{aligned}
&\partial_{t_3} f_i^{\mathrm{eq}}+c_{i\alpha}\partial_\alpha f_i^{(2)}+\partial_{t_1} f_i^{(2)}+\partial_{t_2} f_i^{(1)}\\
&\quad+\tfrac{1}{2}(\underline{\partial_{t_1t_2}+\partial_{t_2t_1}}+2c_{i\alpha}\partial_{t_2\alpha}) f_i^{\mathrm{eq}}\\
&\quad+\tfrac{1}{2}(\partial_{t_1t_1}+2c_{i\alpha}\partial_{t_1\alpha}+c_{i\alpha}c_{i\beta}\partial_{\alpha\beta}) f_i^{(1)}\\
&\quad+\tfrac{1}{6}(\partial_{t_1t_1t_1}+3c_{i\alpha}\partial_{t_1t_1\alpha}+3c_{i\alpha}c_{i\beta}\partial_{t_1\alpha\beta}\\
&\quad+c_{i\alpha}c_{i\beta}c_{i\gamma}\partial_{\alpha\beta\gamma}) f_i^{\mathrm{eq}}\\
&=-\omega f_i^{(3)}.
\end{aligned} \tag{12}$$

Special attention is needed for the underlined terms. Summing the cross derivative $\partial_{t_1t_2} f_i^{\mathrm{eq}}$ in the above equation over i, we get

$$\partial_{t_1t_2}(\rho).$$

It results in two different results by using the first- and second-order equations (8)–(11). (1) If we take the derivative over t_2 first, then $t_1, \partial_{t_2t_1}(\rho)=0$ is obtained; (2) if we take the opposite order, then we have $\partial_{t_1t_2}(\rho)=-\nu\partial_\alpha[\partial_{\beta\beta}(\rho u_\alpha)+\partial_{\alpha\beta}(\rho u_\beta)]$.

It is obvious that these two differential operators are not commutative,

$$\partial_{t_1t_2}(\cdot)\neq\partial_{t_2t_1}(\cdot)$$

where $\cdot$ is either ρ or ρu_α. Fortunately, as it is shown in the lengthy equation (12) that the sum of these two terms is important and all other terms involved can be uniquely determined. After a tedious algebraic calculation, we obtain the third-order ϵ^3 equations,

$$\partial_{t_3}\rho=\frac{c_s^2}{6}\partial_{\alpha\beta\beta}(\rho u_\alpha), \tag{13}$$

$$\partial_{t_3}(\rho u_\alpha)=\frac{c_s^4}{6}\left(\frac{12}{\omega^2}-\frac{12}{\omega}+1\right)\partial_{\alpha\beta\beta}(\rho). \tag{14}$$

The wave vector expansion method has been used by Luo *et al.* [13] for the two-dimensional (2D) Frisch-Hasslacher-Pomeau model and by Coevorden *et al.* [14] for the four-dimensional (4D) face-centered-hyper-cube model. Up to second order of small k there is an agreement of the dispersion relations between the wave vector expansions and the present study.

The final Burnett-like dynamical equations (8) are the following:

$$\partial_t\rho+\partial_\alpha(\rho u_\alpha)=B_0\partial_{\alpha\beta\beta}(\rho u_\alpha), \tag{15}$$

$$\begin{aligned}
\partial_t(\rho u_\alpha)+\partial_\beta(\rho u_\alpha u_\beta)&=-c_s^2\partial_{\alpha\rho}+\nu[\partial_{\beta\beta}(\rho u_\alpha)+\partial_{\alpha\beta}(\rho u_\beta)]\\
&\quad+B_1\partial_{\alpha\beta\beta}(\rho),
\end{aligned} \tag{16}$$

where B_0 and B_1 are dispersion coefficients,

$$\nu=\frac{c_s^2}{2}\left(\frac{2}{\omega}-1\right),\quad B_0=\frac{c_s^2}{6},\quad B_1=\frac{c_s^4}{6}\left(\frac{12}{\omega^2}-\frac{12}{\omega}+1\right). \tag{17}$$

$B_0=\text{const}\neq 0$ comes from the time and space discreteness of lattice-based models. Integrating Eq. (15) over space, the total mass is still conserved, the same is true for the momentum in Eq. (16). Indeed, we can use variable changes, that $\overline{\rho u_\alpha}=\rho u_\alpha-B_0\Delta(\rho u_\alpha)$ (and $\overline{\rho}=\rho$), to make the continuity equation (15) in the usual form, while it is not trivial to figure out the form for the momentum equation.

Higher-order (fourth and up) dynamical equations (super-Burnett-like) [8] can be obtained while tremendous care has to be taken since more noncommutative operators are involved and results will be published elsewhere.

III. DISCRETE KINETIC BGK MODELS IN CONTINUOUS TIME AND SPACE

In finite difference schemes, dispersion terms appear as a numerical artifact without physical soundness. Lattice BGK models can be considered as a variant of a finite difference scheme, and it may be arguable that these dispersion terms are numerical. This is only partially correct since kinetic models with continuous time and space [15] have similar terms as Burnett first worked out more than 60 years ago. In what follows, we outline the results of discrete kinetic BGK models that use the differential form of the evolution equation (1),

$$\partial_t f_i(t,\vec{x})+c_{i\alpha}\partial_\alpha f_i(t,\vec{x})=\omega(f_i^{\text{eq}}-f_i). \tag{18}$$

The same form of equations as Eqs. (15) and (16) is obtained, the only changes come from transport coefficients,

$$\nu=\frac{c_s^2}{\omega},\quad B_0=0,\quad B_1=\frac{2c_s^4}{\omega^2}. \tag{19}$$

These results are independent of any numerical schemes, only the Chapman-Enskog expansion and physical conservations are used.

IV. LINEAR DISPERSION RELATION AND SHOCK CONDITIONS

Neglecting the nonlinear term in Eq. (16) and using the Fourier analysis $\exp^{i(\Omega t-kx)}$ in one dimension (Ω is the complex frequency and k real wave number), we obtain the linear dispersion relation from Eqs. (15) and (16),

$$\Omega^2-i2\nu k^2\Omega-(1+B_0k^2)(c_s^2+B_1k^2)k^2=0. \tag{20}$$

The sound speed is defined as $C_s=\text{Re}(\Omega)/k$ and we get,

$$C_s=\sqrt{(1+B_0k^2)(c_s^2+B_1k^2)-\nu^2k^2}. \tag{21}$$

Numerical simulations will be used to check this formula.

The Rankine-Hugoniot relations across a shock must be satisfied. From the continuity and momentum equations and assuming a moving shock at speed of V_s, these relations read as

$$\rho_1(u_1-V_s)=\rho_2(u_2-V_s), \tag{22}$$

$$\rho_1u_1(u_1-V_s)+c_s^2\rho_1=\rho_2u_2(u_2-V_s)+c_s^2\rho_2, \tag{23}$$

where subscripts 1 and 2 denote the downstream and upstream conditions. After simplification by using the density ratio R (defined as $R=\rho_1/\rho_2$), we have

$$V_s=u_1+\frac{c_s}{\sqrt{R}}, \tag{24}$$

$$u_1-u_2=\frac{R-1}{\sqrt{R}}c_s. \tag{25}$$

V. TRAVELING WAVE ANALYSIS FOR SHOCK STRUCTURE

In Sec. IV we studied the linear dispersion relation by omitting the nonlinear term and the Rankine-Hugoniot relations by ignoring the viscous and dispersive terms. Across a shock wave, both nonlinear and high-order derivatives terms are important and cannot be neglected. We consider one-dimensional cases and assume that a traveling wave solution exists that depends only on $\eta=x-Vt$ (V is the traveling speed that is equal to V_s in the shock wave case). We get the following equations from Eqs. (15) and (16):

$$-\rho V+\rho u-B_0(\rho u)_{\eta\eta}=K_1, \tag{26}$$

$$-\rho uV+\rho u^2+c_s^2\rho-2\nu(\rho u)_\eta-B_1(\rho)_{\eta\eta}=K_2, \tag{27}$$

where K_1 and K_2 are integration constants that depend on boundary conditions. Here we use the shock wave conditions. Two η-independent solutions $\rho=\rho_1$, $u=u_1$ and $\rho=\rho_2$, $u=u_2$ are the two fixed points of the above dynamical Eqs. (26) and (27). Linearizing these equations around fixed points, we get the eigenvalue equation

$$\lambda^4-\left(\frac{1}{B_0}+\frac{1}{B_1}(c_s^2-u_*^2)\right)\lambda^2-\frac{2\nu V}{B_0B_1}\lambda+\frac{1}{B_0B_1}(c_s^2-u_*^2+2u_*V-V^2)=0, \tag{28}$$

where u_* is the steady solution of velocity corresponding to either the downstreaming velocity u_1 or that of upstreaming u_2 of a shock wave. The stability of fixed points depends on the sign of the real part of λ; if the imaginary part of λ is not zero, then an oscillatory solution appears. This fourth-order polynomial equation is difficult to solve and we have to use numerical solutions.

For degenerated systems (either $\nu=0$ or $B_0=0$ or $B_1=0$), we can obtain the analytical criterion determining the boundary between monotonic and oscillatory shocks. For instance, let us consider the continuous time and space discrete kinetic BGK models. With $B_0=0$, we have the eigenvalue equation

$$B_1\lambda^2+2\nu V\lambda-(c_s^2-u_*^2+2u_*V-V^2)=0. \tag{29}$$

The solution is

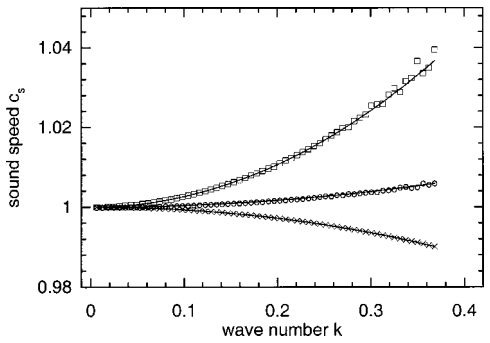

FIG. 1. Dispersion relation: the sound speed c_s vs wave number k using different $\omega=0.75$, 1.00, 1.50. Curves are predictions and points are simulations: □ for $\omega=0.75$, ○ for 1.00, and × for 1.50.

$$\lambda=\frac{-\nu V\pm\sqrt{\nu^2V^2+B_1(c_s^2-u_*^2+2u_*V-V^2)}}{B_1}. \quad (30)$$

The determinant is

$$\Delta=\nu^2V^2+B_1(c_s^2-u_*^2+2u_*V-V^2).$$

We now can study the stability of the two steady solutions with $V=\sqrt{R}c_s$,

$$u_*=u_1=\frac{R-1}{\sqrt{R}}c_s,$$

$$\Delta=\nu^2Rc_s^2+B_1\frac{R-1}{R}c_s^2$$

$$=\frac{R^2+2R-2}{R}\frac{c_s^6}{\omega^2}>\nu^2Rc_s^2>0, \text{ when } R>1.0. \quad (31)$$

This solution is unstable since at least one root of λ is positive.

$$u_*=u_2=0,$$

$$\Delta=\nu^2Rc_s^2+B_1(1-R)c_s^2=(2-R)\frac{c_s^6}{\omega^2}<\nu^2Rc_s^2. \quad (32)$$

The solution is stable since the real part of λ is negative while oscillations appear when $R>2.0$ for the imaginary part of λ is not zero. Otherwise, monotonic shock persists when $1.0<R<2.0$.

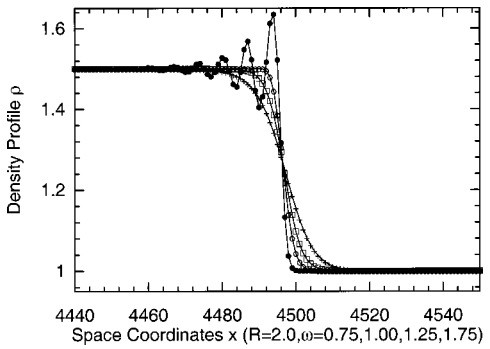

FIG. 2. The density profiles with $R=1.5$ at $t=2000$. Different values of ω are used: + for $\omega=0.75$, □ for 1.00, ○ for 1.25, and ● for 1.75. The model D1Q5 on a lattice of 8192 nodes is utilized.

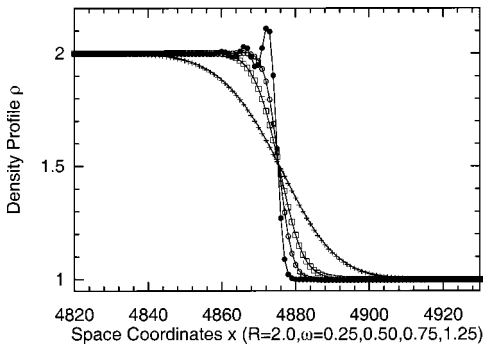

FIG. 3. The density profiles with $R=2.0$ at $t=2000$. Different values of ω are used: + for $\omega=0.25$, □ for 0.50, ○ for 0.75, and ● for 1.25. The model D1Q5 on a lattice of 8192 nodes is utilized.

VI. NUMERICAL RESULTS

We use the one-dimensional five-velocity model (D1Q5) to numerically study the interactions of dissipation and dispersion. The first verification is to measure the dispersion relation (21). Figure 1 shows the sound speed C_s in function of wave number k. Continuous curves are theoretical predictions and points are numerical simulations, a satisfactory agreement is achieved. The deviation of C_s from the dispersionless dynamics can be as high as 4%. In the following simulations, we consider a lattice of 8192 nodes and use the upstreaming density ρ_2, velocity u_2 (=0 for simplicity), and that of downstream ρ_1,u_1. From Sec. V, we have $V=\sqrt{R}c_s$ and $u_1=(R-1/R)c_s$. The initial shock is located at $x=2048$. The control parameters are now the density ratio R characterizing the strength of shock and relaxation parameter ω determining the viscosity v and dispersion coefficient B_1 (B_0 is a constant).

In Fig. 2, the density profile is presented at time $t=2000$ steps for $R=1.5$ and different ω ranging from 0.75, 1.00, 1.25, and 1.75. Monotonic shock wave solutions for $\omega=0.75$, 1.00, 1.25 while oscillatory for $\omega=1.75$ are captured. Figure 3 is similar to Fig. 2 while $R=2.0$ and $\omega=0.25$, 0.50, 0.75, and 1.25. We notice that the higher density ratio R results in more pronounced dispersion effects while comparing these two pictures. It can be easily explained as follows: larger R makes the shock thinner, which in turn causes the third-order dispersion terms to be more effective; these features are very reminiscent of the KdV soliton simulations of Zabusky and Kruskal [16].

In a certain case, we observe an overshoot of density right after the shock. This is shown in Fig. 4 with $R=2.4$, ω

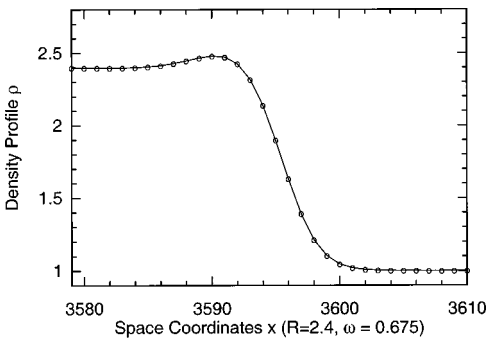

FIG. 4. The density profile with $R=2.4$ and $\omega=0.675$ at $t=1000$. A single hump of density right after the shock is observed.

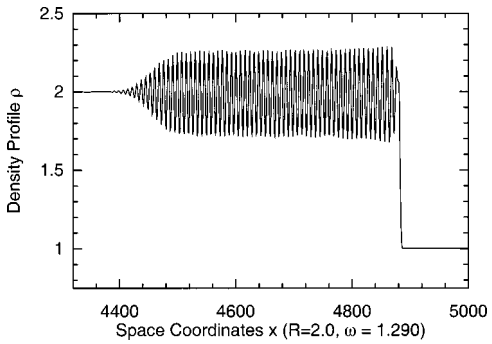

FIG. 5. Density profile with $R=2.0$ and $\omega=1.29$ at $t=2000$. A saturated oscillation after the shock is captured.

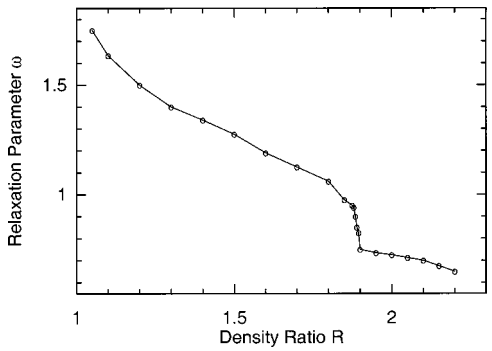

FIG. 6. The relation of density ratio R with the relaxation parameter ω that separates the monotonic shock wave solutions and oscillatory shock wave solutions. A sharp change around $R=1.815$ is numerically found. Above the curve, the solutions are oscillatory solutions, while below it the solutions are monotonic shock wave solutions.

$=0.675$. Appert and d'Humières [17] found a similar density profile when they studied the liquid-gas interface; it was then not quite understood. We suggest that the third-order dispersion might be responsible for it. A natural question to ask is what the density profile looks like if the dispersion is strong. A case with $R=2.0$, $\omega=1.29$ is presented in Fig. 5. Oscillation attains a saturation that is similar to the boundary-generated solitary waves studied by Chu, Xiang, and Baransky by using the KdV equation [18]. In the presence of quadratic nonlinearity, the monotonic shock regime corresponds to the dissipation dominating regime, while the oscillatory solutions correspond to the dispersion effective regime. It would be interesting to find the boundary between these two regimes in the R-ω diagram, the numerical result is shown in Fig. 6. There is a sharp starting around $R=1.815$, which roughly corresponds to $\omega=1.1$ at which B_1 changes its sign.

VII. DISCUSSIONS AND CONCLUDING REMARKS

We reported in this paper the Burnett-like hydrodynamic equations up to third-order for lattice BGK models using the Chapman-Enskog expansion. Great care has been paid to the derivation since the cross time derivatives are not commutative. Linear dispersion relation is obtained and confirmed by numerical simulation. Though the derived equations are quite general, we used a one-dimensional model (D1Q5) to study the interactions of dissipation and dispersion. Using shock wave boundary conditions, two regimes have been observed: monotonic shocks (dissipation dominating) and oscillatory shocks (dispersion effective). The boundary of the two regimes is numerically determined. Density overshoot (humps) and saturation (oscillatory) are also captured as consequences of interactions between nonlinearity, dissipation, and dispersion. Whether or not the newly derived third dispersion terms in two and three dimensions can help us to understand vortex cascades in turbulence is a quite interesting and debatable question.

ACKNOWLEDGMENT

Part of the work was accomplished during a short visit by Y.H.Q. to CNLS of Los Alamos National Laboratory.

[1] U. Frisch, B. Hasslacher, and Y. Pomeau, Phys. Rev. Lett. **56**, 1505 (1986).
[2] U. Frisch, D. d'Humières, B. Hasslacher, P. Lallemand, Y. Pomeau, and J.-P. Rivet, Complex Syst. **1**, 649 (1987).
[3] Y. H. Qian, Ph.D. thesis, ENS, 1990.
[4] Y. H. Qian, D. d'Humières, and P. Lallemand, Europhys. Lett. **17**, 479 (1992).
[5] H. D. Chen, S. Y. Chen, and W. Matthaeus, Phys. Rev. A **45**, R5339 (1992).
[6] *Lattice Gas Methods for Partial Differential Equations*, edited by G. D. Doolen (Addison-Wesley, Reading, MA, 1989.
[7] D. Rothman and S. Zaleski, *Lattice Gas Automata* (Cambridge University Press, Cambridge, England, 1997).
[8] S. Chapman and T. G. Cowling, *The Mathematical Theory of Nonuniform Gases*, 3rd ed. (Cambridge University Press, Cambridge, England, 1970).
[9] R. Benzi, S. Succi, and M. Vergassola, Phys. Rep. **222**, 145 (1992).
[10] Y. H. Qian and S. A. Orszag, Europhys. Lett. **21**, 255 (1993).
[11] Y. H. Qian, S. Succi, and S. A. Orszag, Annu. Rev. Comput. Phys. **3**, 195 (1995).
[12] S. Y. Chen and G. D. Doolen, Annu. Rev. Fluid Mech. **30**, 329 (1998).
[13] L. S. Luo, H. D. Chen, S. Y. Chen, G. D. Doolen, and Y. C. Lee, Phys. Rev. A **43**, 7097 (1991).
[14] D. V. van Coevorden, M. H. Ernst, R. Brito, and J. A. Somers, J. Stat. Phys. **74**, 1085 (1994).
[15] R. Gatignol, *Théorie Cinétique des Gaz à Répartition Discrète de Vitesses*, Lectures Notes in Physics Vol. 36 (Springer-Verlag, New York, 1975).
[16] N. J. Zabusky and M. D. Kruskal, Phys. Rev. Lett. **15**, 240 (1965).
[17] C. Appert and D. d'Humières, Phys. Rev. E **51**, 4335 (1995).
[18] C. K. Chu, L. W. Xiang, and Y. Baransky, Commun. Pure Appl. Math. **36**, 495 (1983).